Journal of Neurochemistry, 2006, **97**, 151–161 doi:10.1111/j.1471-4159.2006.03716.x

Activation of ERK1/2 MAP kinases in Familial Amyloidotic Polyneuropathy

F. A. Monteiro,*,† M. M. Sousa,* I. Cardoso,* J. Barbas do Amaral,‡ A. Guimarães§ and M. J. Saraiva*,†

*Molecular Neurobiology, Instituto de Biologia Celular e Molecular, Porto, Portugal
†ICBAS, University of Porto, Portugal
‡Estomatology, Maxillofacial Surgery, Hospital Geral de Santo António, Porto, Portugal
§Neuropathology, Hospital Geral de Santo António, Porto, Portugal

Abstract

Familial amyloidotic polyneuropathy (FAP) is a neurodegenerative disorder characterized by the extracellular deposition of transthyretin (TTR), especially in the PNS. Given the invasiveness of nerve biopsy, salivary glands (SG) from FAP patients were used previously in microarray analysis; mitogen-activated protein (MAP) kinase phosphatase 1 (MKP-1) was down-regulated in FAP. Results were validated by RT-PCR and immunohistochemistry both in SG and in nerve biopsies of different stages of disease progression. MKP-3 was also down-regulated in FAP SG biopsies. Given the relationship between MKPs and MAPKs, the latter were investigated. Only extracellular signal-regulated kinases 1/2 (ERK1/2) displayed increased activation in FAP SG and nerves. ERK1/2 kinase (MEK1/2) activation was also up-regulated in FAP nerves. In addition, an FAP transgenic mouse model revealed increased ERK1/2 activation in peripheral nerve affected with TTR deposition when compared to control animals. Cultured rat Schwannoma cell line treatment with TTR aggregates stimulated ERK1/2 activation, which was partially mediated by the receptor for advanced glycation end-products (RAGE). Moreover, caspase-3 activation triggered by TTR aggregates was abrogated by U0126, a MEK1/2 inhibitor, indicating that ERK1/2 activation is essential for TTR aggregates-induced cytotoxicity. Taken together, these data suggest that abnormally sustained activation of ERK in FAP may represent an early signaling cascade leading to neurodegeneration.

Keywords: amyloid, extracellular signal-regulated kinases 1/ 2, familial amyloidotic polyneuropathy, mitogen-activated protein kinase phosphatase 1, transthyretin.
J. Neurochem. (2006) **97**, 151–161.

Familial amyloidotic polyneuropathy (FAP) is an autosomal dominant neurodegenerative disorder characterized by the extracellular deposition of transthyretin (TTR) amyloid fibrils throughout the connective tissue of several organs, particularly in the peripheral nervous system (PNS) (Coimbra and Andrade 1971a,b). Morphologically, FAP is characterized by distal axonal loss of fibers that leads to the pathophysiological condition associated with this disorder. In FAP, the most common TTR variant presents a substitution of methionine for valine at position 30 – TTR V30M. In the peripheral nerve, TTR aggregates and amyloid fibrils appear mainly in the endoneurium in proximity of blood vessels and near Schwann cells (SC) and collagen fibrils (Coimbra and Andrade 1971a,b). In latter stages of disease progression, severely affected nerves present endoneurium contents replaced by amyloid, abundant collagen bundles, SC without axons and fibroblasts, and only a few nerve fibers retain viability. In ganglia, TTR amyloid deposits are present in the stroma in close contact with satellite cells and a progressive loss of neurons is observed (Hofer and Anderson 1975; Ikeda *et al*. 1987; Hanyu *et al*. 1989; Takahashi *et al*. 1991).

Received September 19, 2005; revised manuscript received November 22, 2005; accepted December 12, 2005.

Address correspondence and reprint requests to Maria João Saraiva IBMC- Molecular Neurobiology, R. Campo Alegre, 823. 4150–180 Porto, Portugal. E-mail: mjsaraiv@ibmc.up.pt

Abbreviations used: ERK, extracellular signal-regulated kinase; FAP, familial amyloidotic polyneuropathy; iNOS, inducible nitric oxide synthase; IL-1β, interleukin-1β; MKP-1, MAPK phosphatase 1; MEK, MAPK/ERK kinase; MCSF, macrophage-colony stimulating factor; NFkB, nuclear transcription factor kB; pERK, phosphorylated ERK; pMEK, phosphorylated MEK; RAGE, receptor for advanced glycation end-products; SG, salivary gland; SAPK/JNK, stress-activated protein kinase or jun amino-terminal kinase; tERK, total ERK; tMEK: total MEK; TTR, transthyretin; TNFα, tumor necrosis factor α.

Recently, it was shown that TTR aggregates bind to the receptor for advanced glycation end-products (RAGE) and that FAP tissues have increased expression of this receptor in sites related to amyloid deposition (Sousa *et al*. 2000). The TTR aggregates–RAGE interaction exerts cytotoxic effects as it triggers activation of the nuclear transcription factor kB (NFkB) (Sousa *et al*. 2000). FAP nerves show increased expression of proinflammatory cytokines such as tumor necrosis factor α (TNFα), interleukin-1β (IL-1β) and macrophage-colony stimulating factor (MCSF). Oxidative stress also arises in FAP nerves by up-regulation of inducible nitric oxide synthase (iNOS) (Sousa *et al*. 2001a), which produces NO. Furthermore, caspase-3, a critical protease in the late execution phase of apoptosis, was shown to be up-regulated in axons of FAP nerves. Activation of these markers was abrogated in cell culture by an anti-RAGE antibody or by the soluble domain of RAGE.

These studies represented the first step to understand the involvement of RAGE in the pathophysiological changes in FAP. The signaling mechanisms that mediate TTR aggregates–RAGE interaction and NFkB activation are presently unknown. The engagement of RAGE by a ligand triggers activation of key cell signaling pathways, such as p21ras, mitogen-activated protein kinases (MAPKs), NF-kB and cdc42/rac, thereby reprogramming cellular properties (Yan *et al*. 1994; Lander *et al*. 1997; Huttunen *et al*. 1999). For example, the inhibition of RAGE–amphoterin interaction suppressed activation of extracellular signal-regulated kinase 1/2 (ERK1/2), p38 and stress-activated protein kinases or jun amino-terminal kinases (SAPKs/JNKs) MAPKs in rat C6 glioma cells (Taguchi *et al*. 2000).

ERK1/2 are serine-threonine kinases and are activated by dual phosphorylation of threonine and tyrosine residues at the activation domain carried out by MAPK kinase 1/2 (MEK1/2) (Pearson *et al*. 2001). Active-ERK1/2 targets include several transcription factors, signaling mediators, cytoskeletal proteins and protein kinases. Because ERK1/2 substrates are found in various subcellular compartments (Grewal *et al*. 1999), the biological outcome of ERK1/2 activation will depend in part of the localization of ERK1/2 and its accessibility to potential substrates within that compartment. ERK1/2 cytoplasmic substrates are of particular importance in neurons, in which ERK1/2 activation may occur at a considerable distance from the nucleus. ERK1/2 activity is decreased by either phosphotyrosine phosphatases or dual specificity (serine-threonine and tyrosine) phosphatases also known as MAPK phosphatases (MKPs) (Pearson *et al*. 2001).

Differential gene expression microarray data from human FAP salivary glands (SG) has shown differences in genes expressed in control and FAP SG, which included extracellular matrix (ECM) remodelling genes; microarray results were validated in nerve biopsies (Sousa *et al*. 2005). In the microarray data, MAPK phosphatase 1 (MKP-1/CL100) expression was 6-fold down-regulated in FAP. MKP-1 is an inducible nuclear dual specificity phosphatase that can dephosphorylate and inactivate ERK1/2, SAPK/JNK and p38 MAPKs (Camps *et al*. 2000).

In the present study we questioned whether MKPs and MAPKs are associated with FAP pathology.

Materials and methods

Subjects

Labial minor salivary glands (SG) biopsies were obtained from V30M FAP patients prior to performing liver transplantation, the only available treatment for this disorder. Control SG were from age- and gender-matched non-FAP volunteer individuals that had no evidence of infection. The collection of biopsies material was approved by ethical committee of Hospital Geral de Santo António, Porto, Portugal, and participant subjects were volunteers. SG collection and characterization was described previously (Sousa *et al*. 2005). For immunohistochemical analysis, SG were collected to 4% paraformaldehyde in phosphate-buffered saline (PBS). The general characterization of SG consisted of TTR immunohistochemistry and analysis of presence of amyloid deposits by Congo red staining. SG with TTR deposition but without amyloid deposits were classified as FAP 0, and SG with TTR deposition along with amyloid deposits were classified as FAP. Sural nerve biopsy specimens from FAP patients, asymptomatic carriers (FAP 0) and controls (near relatives of FAP patients who ultimately turned out not to have mutations in TTR) were available at the Hospital Geral de Santo António, Porto, Portugal, since this material was obtained as part of the clinical diagnosis and evaluation of FAP, prior to the current use of molecular diagnostic methods.

Microarray and semi-quantitative RT-PCR analysis

Salivary glands from four FAP patients and four control individuals, age and gender matched, were collected and hybridization to the U95A oligonucleotide array (Affymetrix, Memphis, TN, USA) which represents ~12 000 human sequences was performed as described in Sousa *et al*. (2005). Genes scored as increased or decreased in all pairwise comparisons were selected. A gene was considered to have modified expression if it averaged ≥ ± 2.5 fold change. In this analysis we found down-regulation (6.2-fold ± 1.4) of mitogen-activated protein (MAP) kinase phosphatase 1 (MKP-1/CL100). To validate the microarray data at the RNA level, total RNA from salivary glands from 3 control individuals and 3 FAP patients was isolated with Trizol (Invitrogen, Carlsbad, CA, USA) and subjected to RT-PCR with the Superscript II kit (Invitrogen). PCR was performed for 30 cycles at 95°C for 30 s, 56°C for 45 s and 72°C for 1 min. Specific primers were designed using PRIMER3 (http://frodo.wi.mit.edu/cgi-bin/primer3/primer3_www.cgi) and the sequence from the National Centre for Biotechnology Information database. Sense and antisense primers were: for human MKP-1, 5′-CTTGATCAACGTCTCAGCCA-3′ and 5′-AGAGGTCGTAATGGGGCTCT-3′ and for human β-actin, 5′- AGAAAATCTGGCACCACACC-3′ and 5′-CCATCTCTTGCTCGAAGTCC-3′. PCR products were quantified from 1% agarose gels by densitometry using the Scion Image software (Scion Corporation). Density values of RT-PCR products were normalized with β-actin PCR product. Results are presented as normalized density ± SD.

Immunohistochemistry

For immunohistochemical analysis, nerve and SG paraffin sections were deparaffinated, hydrated in a modified alcohol series, antigens were unmasked by microwaving in 10 mM sodium citrate buffer pH 6.0, endogenous peroxidase activity was blocked with 3% hydrogen peroxide in methanol for 15 min and incubated in blocking buffer (4% fetal bovine serum (FBS) and 1% bovine serum albumin (BSA) in PBS) for 30 min at 37°C in a moist chamber. Incubation with primary antibody, at the appropriate dilution in blocking buffer, was performed overnight at 4°C in a humidified chamber. Primary antibodies were rabbit polyclonal anti-phospho-MEK1/2 (Ser217/221) 1 : 50-nerves; 1 : 100-SG, rabbit polyclonal anti-MEK1/2 (1 : 100-nerves), mouse monoclonal anti-phospho-p44/42 MAP kinase (Thr202/Tyr204) 1 : 20-nerves; 1 : 100-SG, rabbit polyclonal anti-p44/42 MAP kinase (1 : 100-nerves and SG), mouse monoclonal anti-phospho-p38 (Thr180/Tyr182) 1 : 20-nerves; 1 : 50-SG, mouse monoclonal anti-phospho-JNK/SAPK (Thr183/Tyr185) 1 : 20-nerves; 1 : 50-SG, all purchased from Cell Signaling Tecn. (Frankfurt, Germany); rabbit polyclonal anti-MKP-1 (V-15) 1 : 100-nerves; 1 : 500-SG, goat polyclonal anti-MKP-3 (N-18) 1 : 20-nerves; 1 : 100-SG, mouse monoclonal anti-phospho-JNK (G-7); 1 : 20-nerves were from Santa Cruz Biotech (Santa Cruz, Heidelberg, Germany). Antigen visualization was performed with either biotin-extravidin-alkaline phosphatase or biotin-extravidin-peroxidase kits (Sigma, St Louis, MO, USA), using Fast Red (Sigma) or 3-amino-9-ethyl carbazole (Sigma), respectively, as substrates. On parallel control sections, primary antibody was replaced by blocking buffer alone. Subsequent immunohistochemistry was performed with either affinity-purified alkaline phosphatase- or peroxidase- conjugated secondary antibody (Sigma). Semiquantitative immunohistochemistry (SQ-IHC) analysis was performed using Scion Image software (freely downloaded from Scion Corporation website). This application enables the measurement of the area occupied by pixels corresponding to the immunohistochemical substrate's color that is normalized relatively to the total area. Each slide used in the SQ-IHC was analyzed in 5 different representative areas. To assess kinase activation, data is shown as the ratio between the stained areas occupied by phospho-specific and total-specific antibodies, within the same nerve biopsy. Results shown represent percentage occupied area (± SD).

Proteins

Wild type recombinant TTR was produced from *E. coli* BL21 expression system and purified as previously described (Almeida *et al*. 1997). Purified soluble TTR was detoxified using Endotoxin Removing Gel (Pierce, Rockford, IL, USA). For preparation of TTR aggregates, TTR was dialyzed against water, pH 7.0, and then incubated with 0.05 M sodium acetate, pH 3.6, for 48 h at 22°C. The preparation was then centrifuged at 15 000 *g* for 30 min, the pellet washed and resuspended in PBS, pH 7.4. Protein concentration was determined by the Lowry method (Lowry *et al*. 1951). TTR aggregates are composed of short fibrils and amorphous aggregates as assessed by ultrastructural analysis (Sousa *et al*. 2001b).

Cell culture assays

RN22 cells (rat Schwannoma cell line) were from the European Collection of Cell Cultures. RN22 were propagated in 10 cm dishes in monolayer and maintained at 37°C in a humidified atmosphere of 95% and 5% CO_2. Cells were grown in Dulbecco's minimal essential media (DMEM) (Gibco, Rockville, MD, USA) supplemented with 10% FBS (Gibco), 2 mM glutamine (Sigma) and 100 U/mL penicillin/streptavidin (Gibco) (complete media). For ERK1/2 activation assays, cells were grown in complete media in six-well plates. When ~50% confluence was reached, cells were washed with PBS and starved in DMEM containing 1% dialyzed FBS for ~16 h. Subsequently, cells were treated with 1 μM of soluble or aggregated TTR for the indicated time periods. For studies using goat polyclonal anti-RAGE antibody (N-16) (α-RAGE) (Santa Cruz Biotech) and non-immune (NI) purified IgGs from goat serum (Sigma), following starvation, cells were preincubated for 3 h with 30 μg/mL of αRAGE or NI, and then treated with 1 μM TTR aggregates plus 10 μg/mL of αRAGE or NI in DMEM containing 0.5% dialyzed FBS for 30 min. For caspase-3 activation assays, cells were grown in 25 cm^2 flasks. Activation of caspase-3 was measured using the fluorometric caspase-3 assay kit (Sigma), following the manufacturer's instructions. Briefly, 80% confluent cells were incubated in assay media (DMEM containing 1% dialyzed FBS) with 2 μM of soluble or aggregated TTR for 24 h. Where indicated cells were pre-incubated for 1 h with 1 μM U0126 (Calbiochem), a MEK1/2 inhibitor, and subsequently cells were incubated with 5 μM U0126 alone or 5 μM U0126 with 2 μM TTR aggregates. Next, cells were trypsinized and the cell pellet was lysed in 100 μL of kit lysis buffer; 40 μL of each cell lysate sample was used in duplicates for determination of caspase-3 activation. The remaining cell lysate was used to determine total cellular protein concentration with the Bio-Rad protein assay, using BSA as standard. Values shown are the mean of quadruplicates of two independent experiments. Student's *t*-test statistical analysis was used to determine statistical significance between cells exposed to assay media and cells exposed to different regulators.

Immunoblots

Following treatment with TTR, cells were washed twice with ice-cold PBS, and lysed with 100 μL of lysis buffer (Cell Signaling Tecn.) containing a protease inhibitor cocktail (Calbiochem, San Diego, CA, USA). Cell lysates were centrifuged at 11 000 *g* and protein in the supernatant was quantified with the Bio-Rad protein assay. Equal amounts of protein were loaded in 12% SDS–PAGE and transferred to nitrocellulose Hybond-C Extra (Amersham Biosciences, Little Chalfont, Buckinghamshire, UK) using a semidry transfer system. Blots were incubated with blocking buffer (5% non-fat dried milk, and 50 mM NaF, to inhibit phosphatases, in Tris buffered saline (TBS) with 0.1% Tween-20 (T)) for 1 h at room temperature (RT). Subsequently, incubation with primary antibodies, at the appropriate dilution, was performed overnight at 4°C in 5% BSA/TBS-T with 50 mM NaF. The primary antibodies used were rabbit polyclonal anti-phospho-p44/42 MAP kinase (Thr202/Tyr204) 1 : 1000, rabbit polyclonal anti-p44/42 MAP kinase (1 : 1000), purchased from Cell Signaling Tecn., and rabbit polyclonal anti-ERK 1 (C-16) 1 : 1000 from Santa Cruz Biotech. After incubation with secondary sheep anti-rabbit IgGs peroxidase conjugate (1 : 5000) (The Binding Site) in 1% non-fat dried milk TBS-T for 1 h RT, blots were developed using the SuperSignal West Pico Chemiluminescent Substrate kit (Pierce) and exposed to Hyperfilm ECL (Amersham Bioscieneces). Blots were first incubated with phospho-specific antibodies, stripped with Re-Blot Plus

Mild Solution (Chemicon) according to manufacturer's instructions, reblocked, and then incubated with the respective anti-total protein antibody for total protein normalization. Quantitative analysis of immunoblot images was performed using the Scion Image software (Scion Corporation). Results are shown as the squared pixels ratio between phospho-p44/42 MAPK and total-p44/42, and represented as fold activation relatively to cells exposed to assay media.

Nerve preparation

Transgenic mice bearing the human TTR V30M in a TTR-null background (Kohno *et al*. 1997), were compared to TTR-null (Episkopou *et al*. 1993) and wild type mice. Mice were killed by cervical distension. Nerves were rapidly excised and frozen in dry ice. In order to analyze ERK1/2 activation, peripheral nerves were ground into powder with a frozen pestle in dry ice and homogenized in lysis buffer (5 mM EDTA, 2 mM EGTA, 20 mM MOPS pH 7.0, 30 mM sodium fluoride, 20 mM sodium pyrophosphate, 1 mM sodium orthovanadate, 40 mM β-glycerophosphate, 0.5% triton X-100, pH 7.2) supplemented with protease inhibitor cocktail set III (Calbiochem). Homogenate samples were centrifuged at 16 000 *g* for 30 min, and supernatants assayed for protein concentration by the Bio-Rad method.

Statistical analysis

Group values, expressed as the mean ± SD, were compared by Student's *t*-test, and *p*-values of less than 0.05 were considered significant.

Results

MKP-1 and MKP-3 expression is down-regulated in FAP

Gene expression microarray data from human FAP salivary glands (SG) showed down-regulation (6.2-fold ± 1.4) of mitogen-activated protein (MAP) kinase phosphatase 1 (MKP-1/CL100). We validated the microarray data both by RT-PCR and semi-quantitative immunohistochemistry. RT-PCR of MKP-1 mRNA in human SG indicated a down-regulated expression in FAP when compared to controls, as shown in Fig. 1a and chart, confirming the microarray results. By semi-quantitative immunohistochemistry, amyloid laden SG from FAP patients showed a significant down-regulation of MKP-1 (Fig. 1b upper panels and chart), validating the microarray results. MKP-1 immunostaining was more abundant in the cytoplasm of the stratified cuboidal epithelial lining present in excretory ducts than in the nucleus. We then performed immunohistochemical analysis for MKP-1 in FAP nerve biopsies in different stages of disease progression. At later stages of FAP progression, when compared with controls and asymptomatic carriers (FAP 0), MKP-1 expression was down-regulated in axons (as documented in Fig. 1b lower panels and chart). To test whether the expression of other dual specificity MAP kinase phosphatases (MKPs) could be affected in FAP, we studied MKP-3, which specifically inactivates ERK1/2 when compared with JNK and p38 MAPKs. MKP-3 was down-regulated in FAP 0 SG as well as in SG from FAP patients (Fig. 1c upper panels and chart). The immunostaining was exclusively cytoplasmatic in the epithelial lining of excretory ducts. However, in human nerve biopsies, MKP-3 was up-regulated in axons of the FAP 0 asymptomatic stage as compared to controls, but MKP-3 levels at the symptomatic stage did not differ from controls (Fig. 1c lower panels and chart).

ERK1/2 activation is up-regulated in FAP

The diminished expression of MKPs in FAP suggests that MAPKs cascades might be up-regulated in FAP. Semi-quantification of MAPKs by immunohistochemistry of FAP SG did not show activation of p38 and JNK MAPKs when compared to control SG (data not shown). However, ERK1/2 MAPK activation in FAP SG showed a marked up-regulation beginning at FAP 0 and persisting in the FAP stage. Often phosphorylated ERK1/2 (pERK1/2) translocation to the nucleus of stratified cuboidal epithelial lining in excretory ducts was observed, whereas in controls a cytoplasmic localization was present (Fig. 2a and chart). MAPKs were also assessed in human FAP nerve biopsies. Consistently with the analyses of human SG, intensity of immunostaining for phosphorylated forms of p38 and JNK was not statistically different in FAP and control nerves (data not shown). However, increased ERK1/2 phosphorylation was evident in human FAP nerves. In asymptomatic carriers (FAP 0), activated ERK1/2 was approximately 3-fold increased in axons, whereas pERK1/2 was almost absent in controls. Total ERK1/2 (tERK1/2) levels were similar in the two types of samples (Fig. 2b and chart). At a later symptomatic stage, phosphorylation levels of ERK1/2 were lower, however, tERK1/2 levels also decreased, leading to a sustained ERK1/2 activation, when compared to normal specimens (Fig. 2b and chart). ERK1/2 was observed in several cell types, neuronal axons were the main cellular structure with positive staining. These results correlate well with the decreased expression of MKP-1 seen in nerves from FAP patients. Up-regulation of ERK1/2 detected in asymptomatic carriers is not explained by the actions of MKP-1 and -3 and additional mechanisms might intervene at this stage, such as MEK1/2 activation. In an attempt to analyze ERK1/2 activation *in vivo*, we used a transgenic mouse model that expresses human TTR V30M in a TTR-null background. These mice when older than 9 months of age develop TTR amyloid deposits in several organs within the gastrointestinal tract, and at the age of 24 months the pattern of amyloid deposition is similar to the one seen in FAP autopsies except for the absence of TTR deposition in the peripheral nerve (Takaoka *et al*. 1997). When we analyzed protein extracts from TTR V30M mice peripheral nerve, we found a 2-fold increased activation of ERK1/2 in older animals (17 months of age) when compared with younger ones (2 months of age; Fig. 2c). The observed activation was not age-dependent,

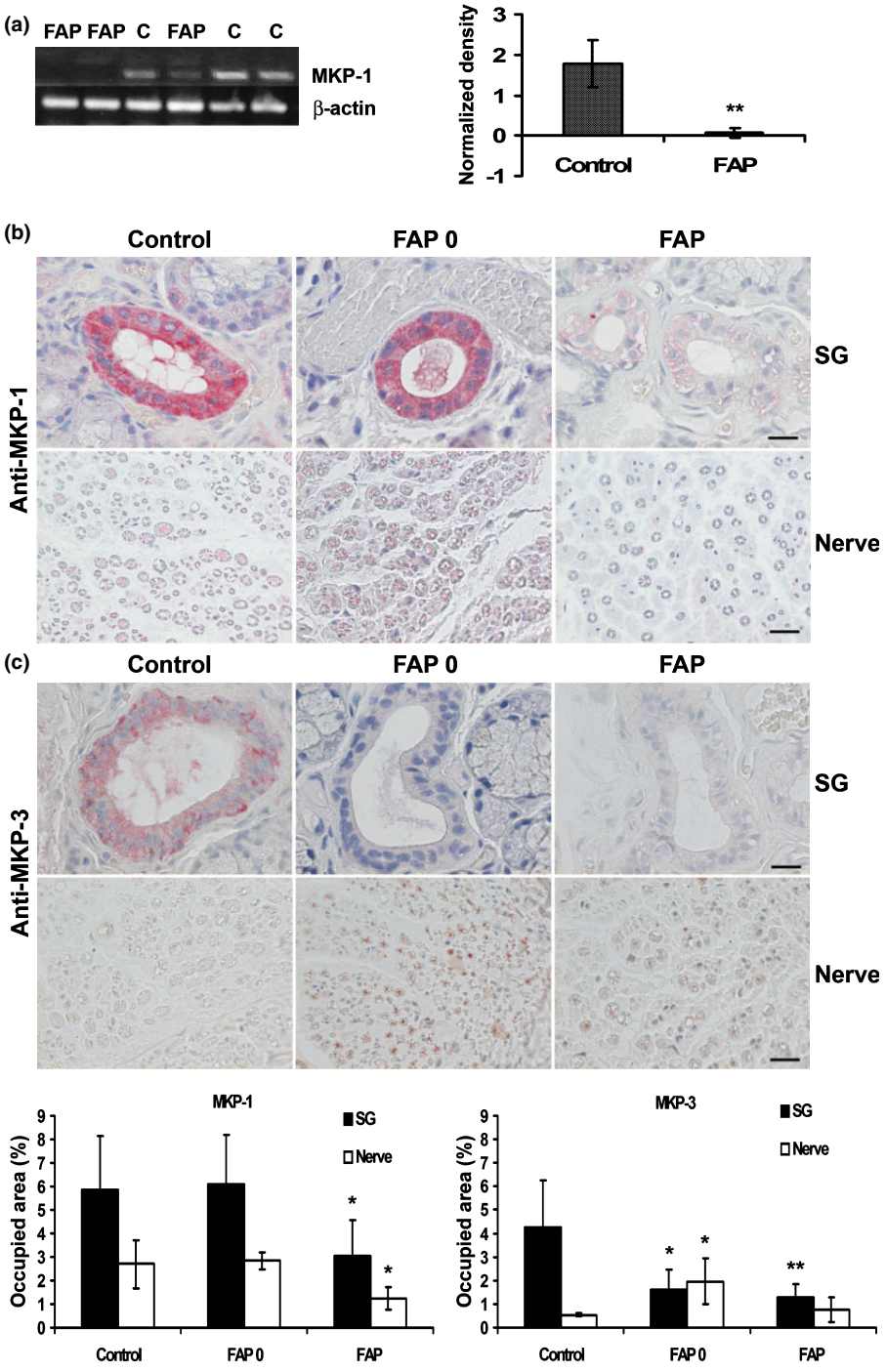

Fig. 1 MKP-1 and MKP-3 expression in FAP. (a) RT-PCR analysis of RNA extracted from salivary glands of control (C) individuals and FAP patients. MKP-1 (upper lane) and β-actin (lower lane). Chart, Densitometry of MKP-1/β-actin RT-PCR amplifications in control ($n = 3$) and FAP ($n = 3$) SG biopsies. $^{**}p < 0.008$, compared to control group. (b) MKP-1 immunohistochemistry of representative SG (upper panels) and nerves (lower panels) from control individuals (left panels), FAP 0 (middle panels) and FAP patients (right panels). Bar, 20 μm. Chart (MKP-1), Quantitation of immunohistochemical images of MKP-1 staining in SG excretory ducts and nerves. (c) MKP-3 immunohistochemistry of representative SG (upper panels) and nerves (lower panels) from control individuals (left panels), FAP 0 (middle panels) and FAP patients (right panels). Bar, 20 μm. Chart (MKP-3), Quantitation of immunohistochemical images of MKP-3 staining in SG excretory ducts and nerve. Data are represented as percentage of occupied area ± SD for SG controls ($n = 6$), FAP 0 ($n = 4$) and FAP patients ($n = 6$), and for nerves controls ($n = 4$), FAP 0 ($n = 6$) and FAP patients ($n = 5$). $^{*}p < 0.05$ and $^{**}p < 0.02$, compared to control groups.

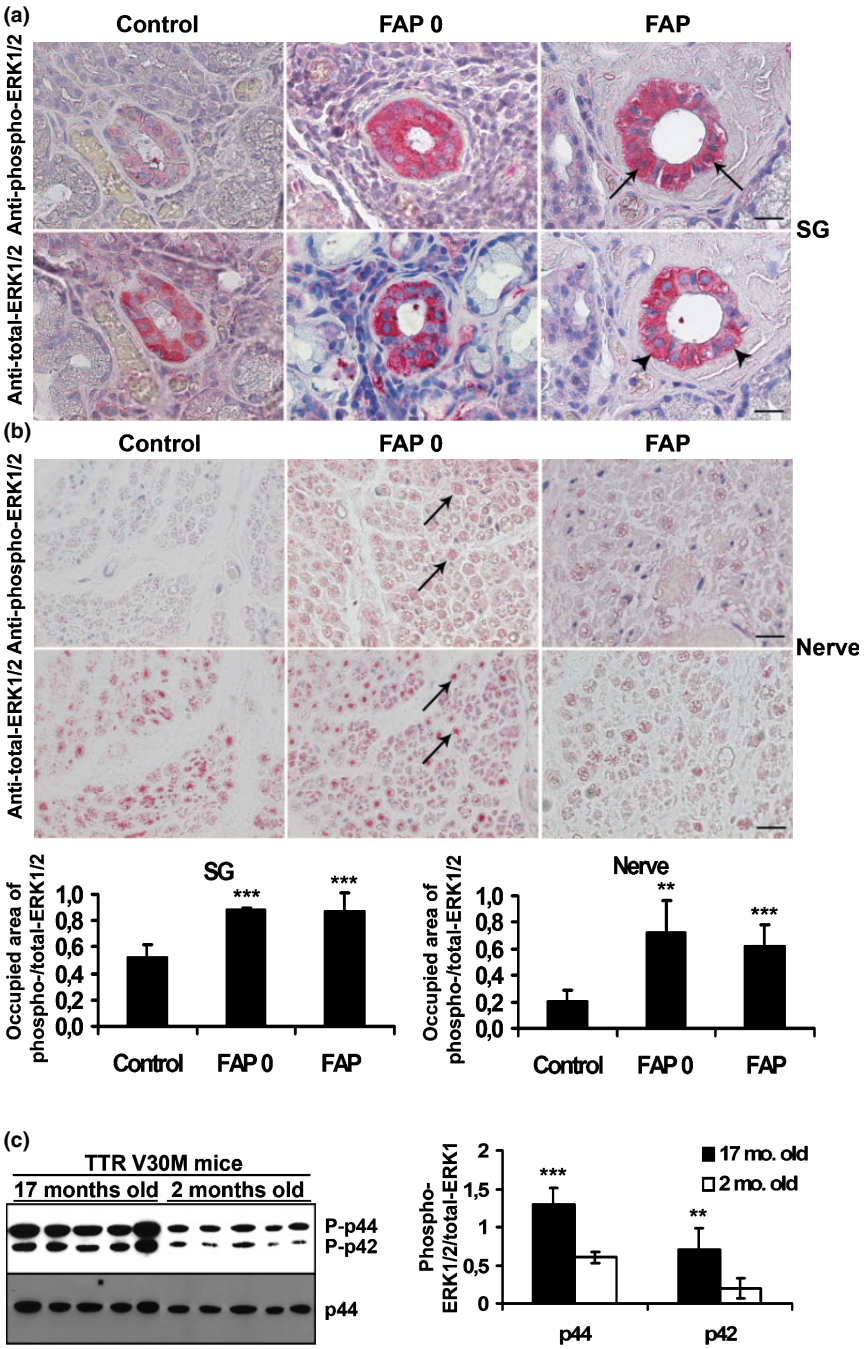

Fig. 2 ERK1/2 increased activation in FAP. (a) Representative pERK1/2 (upper panel) and tERK1/2 (lower panel) immunohistochemistry of SG biopsies from control individuals (left panel), FAP 0 (middle panel) and FAP patients (right panel). Arrows, nuclear translocation. Arrow heads, cytoplasmic localization. Bar, 20 μm. Chart (SG), Quantitation of immunohistochemical images of the ratio between pERK1/2 and tERK1/2 staining in control individuals ($n = 5$), FAP 0 ($n = 3$) and FAP patients ($n = 6$) SG excretory ducts. Data are represented as occupied area in squared pixels ± SD. ***$p < 0.001$. (b) Representative pERK1/2 (upper panel) and tERK1/2 (lower panel) immunohistochemistry of nerves from control individuals (left panel), FAP 0 (middle panel) and FAP patients (right panel). Bar, 20 μm. Chart (Nerve), Quantitation of immunohistochemical images of the ratio between pERK1/2 and tERK1/2 staining in control individuals ($n = 5$), FAP 0 ($n = 7$) and FAP patient ($n = 5$) nerves. Data are represented as occupied area in squared pixels ± SD. **$p < 0.002$, ***$p < 0.001$. (c) ERK1/2 activation in TTR V30M mice peripheral nerve; Immunoblots representing stimulation of pERK1/2 (top lanes) and expression of tERK1 (bottom lane) from peripheral nerve extracts of TTR V30M mice. 20 μg of total protein was loaded per lane. Chart: quantitation of immunoblot images of the ratio between phospho-ERK1/2 (*p*-p44/42) and total-ERK1 (p44). **$p < 0.007$ and ***$p < 0.0001$, comparing older ($n = 6$) to younger ($n = 6$) TTR V30M mice.

since age-matched wild type and TTR-null mice did not show differences on ERK1/2 activation (data not shown). It is possible that low amounts of pre-fibrillar TTR species are present in old transgenic TTR V30M mice not detected by immunohistochemistry. Taken together, the human and mice data point to ERK1/2 up-regulation in FAP tissues.

MEK1/2 activation is up-regulated in FAP

One of the signaling mechanisms that up-regulates ERK1/2 activity are upstream kinases. The immediate upstream ERK1/2 kinase is MEK1/2. Consistent with the human nerve ERK1/2 data, we found MEK1/2 activation (phospho/total levels) up-regulated in FAP nerves both from asymptomatic carriers and patients, relatively to controls (Fig. 3 and chart). As observed for ERK1/2, in a later symptomatic stage, phosphorylation levels of MEK1/2 decreased; however, tMEK1/2 levels were also lower, leading to sustained MEK1/2 activation, when compared to normal specimens. To note that axonal staining is significantly decreased for tERK1/2 and tMEK1/2 due to severe loss of nerve fibers in patients.

ERK1/2 activation is RAGE mediated

The RN22 cellular system, that presents a Schwann cell like phenotype and was previously demonstrated to display RAGE mediated neurotoxicity triggered by TTR aggregates (Sousa *et al*. 2001a), was used to determine whether TTR aggregates could activate the ERK1/2 MAPK cascade. We found that treatment of RN22 cells with TTR aggregates triggered a rapid and sustained ERK1/2 phosphorylation after 15 min, while soluble TTR had no effect (Fig. 4a). Then, we posed the question whether RAGE was mediating ERK1/2 activation stimulated by TTR aggregates. In fact, we found that TTR aggregates-induced ERK1/2 activation was RAGE mediated, as anti-RAGE IgG had a significant inhibitory effect in ERK1/2 activation, when compared with non-immune IgG at the same concentration [Fig. 4b and charts (i) (ii)]. Previous studies demonstrated that prolonged exposure of RN22 cells to TTR aggregates (24 h) leads to a RAGE-dependent activation of caspase-3 (Sousa *et al*. 2001a). Here, we investigated whether ERK1/2 is mediating intracellular signaling leading to induction of apoptosis stimulated by TTR aggregates. Using the described cell culture apoptosis assay (Sousa *et al*. 2001a) we blocked the ERK1/2 signaling pathway with U0126, a MEK1/2 pharmacological inhibitor. U0126 completely abolished TTR aggregates-dependent caspase-3 activation, whereas control U0126 and soluble TTR did not activate caspase-3 (Fig. 4c).

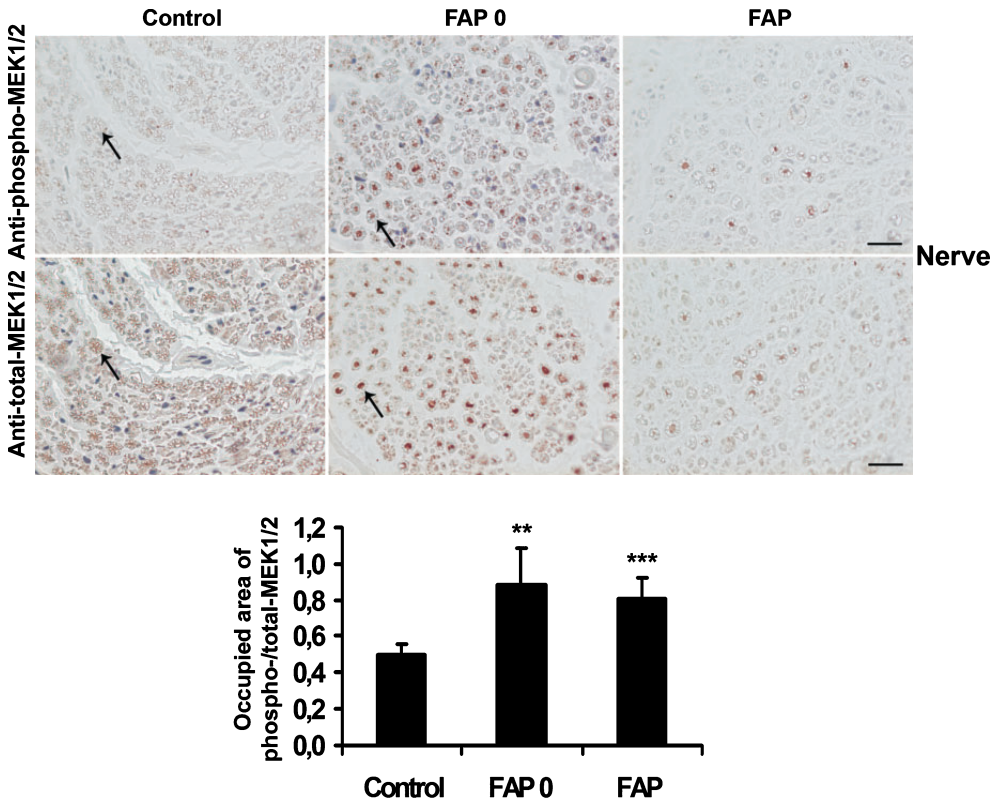

Fig. 3 MEK1/2 increased activation in FAP nerves. pMEK1/2 (upper panels) and tMEK1/2 (lower panels) immunohistochemistry of representative nerves from control individuals (left panels), FAP 0 (middle panels) and FAP patients (right panels). Bar, 20 μm. Chart, Quantitation of immunohistochemical images of the ratio between pMEK1/2 and tMEK1/2 staining in control individuals ($n = 5$), FAP 0 ($n = 7$) and FAP patients ($n = 6$). Data are represented as occupied area in squared pixels ± SD. $^{**}p < 0.01$ and $^{***}p < 0.001$.

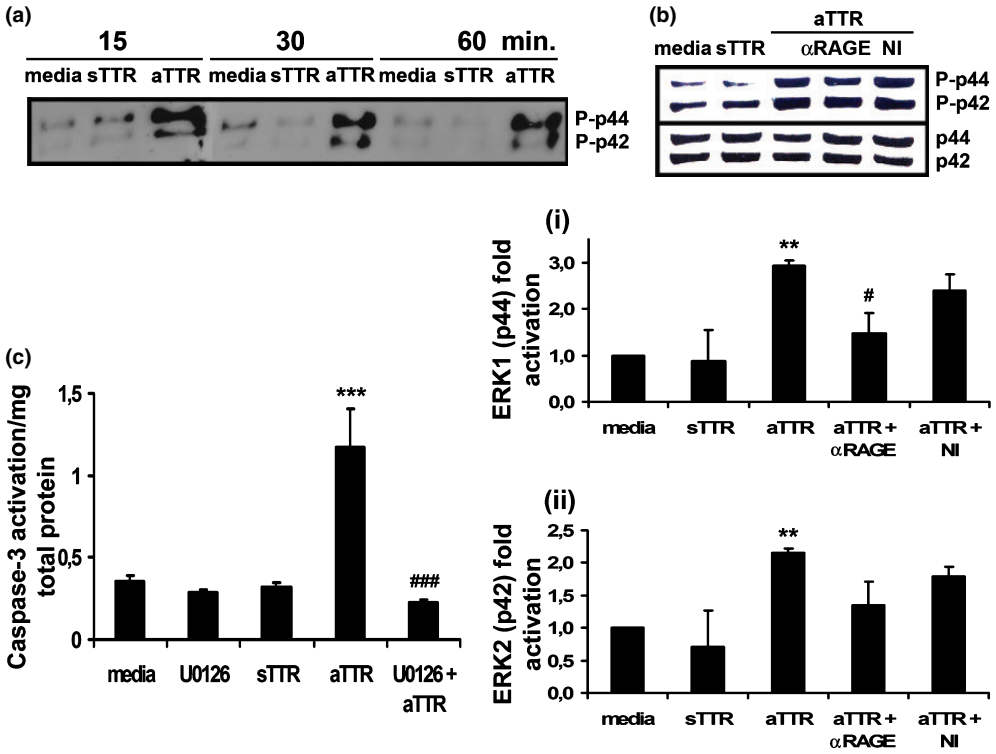

Fig. 4 ERK1/2 activation by TTR aggregates. (a) TTR aggregates trigger ERK1/2 MAPK activation. Immunoblot representing pERK1/2 (*p*-p44/42) induction in RN22 cells exposed for the indicated time periods to either 1 μM soluble TTR (sTTR) or 1 μM TTR aggregates (aTTR). (b) TTR aggregates activate ERK1/2 MAPK cascade via RAGE. Immunoblots representing stimulation of phospho-ERK1/2 (*p*-p44/42) and expression of total-ERK1/2 (p44/42) from RN22 cell lysates. Cells were exposed 30 min to either 1 μM soluble TTR (sTTR) or 1 μM TTR aggregates (aTTR). Where indicated, cells were pre-incubated with polyclonal anti-RAGE (αRAGE) or non-immune IgG (NI). Chart (i): quantitation of immunoblot images of the ratio between phospho- and total-ERK1 (p44), and (ii) phospho- and total-ERK2 (p42). Data are represented as fold activation relatively to non-treated cells (media), which was set as 1. Results derive from three independent experiments. $^{**}p < 0.003$, compared with non-treated cells and $\#p < 0.05$, compared with cells treated with aTTR in the presence of non-immune IgG (aTTR + NI). (c) TTR aggregates induction of caspase-3 is ERK1/2 MAPK mediated. Activation of caspase-3 in RN22 cells exposed for 24 h to either 2 μM soluble TTR (sTTR) or 2 μM aggregated TTR (aTTR). Where indicated cells were pre-incubated with 1 μM U0126 for 1 h. Then these cultures were exposed for 24 h to aTTR (2 μM) along with 5 μM U0126. $^{***}p < 0.001$, compared with non-treated cells (media). $\#\#\#p < 0.001$, compared with cells treated with TTR aggregates.

Discussion

This study addresses early intracellular signaling events occurring as a consequence of TTR deposition in FAP. We propose that the MEK–ERK MAPK signaling pathway is involved in FAP pathogenesis. Supporting this hypothesis, we show that cultured Schwann-like cells treated with TTR aggregates elicit a sustained ERK1/2 activation, which is transduced in part by RAGE. It is possible that other still unknown receptors intervene in the TTR aggregates-induced signaling cascades. It is well characterized that RAGE signaling induces oxidative stress and activates ERK cascades, leading to downstream increased NFκB activity (Yan *et al*. 1994; Lander *et al*. 1997). In addition, the RAGE promoter contains 2 functional NFκB binding sites (Li and Schmidt 1997), therefore both the increased NFκB activation and increased RAGE expression observed in FAP (Sousa *et al*. 2000; Sousa *et al*. 2001a) most likely contribute to the observed ERK sustained activation observed in this cellular system. Moreover, it was demonstrated that the cytosolic domain of RAGE directly binds to ERK by a D-domain docking site (Ishihara *et al*. 2003). *In vivo*, using transgenic mice expressing a signaling transduction deficient RAGE in peripheral neurons, a diminished phosphorylation of ERK1/2 after nerve crush injury has been observed (Rong *et al*. 2004). As shown previously, long exposure of RN22 cells to TTR aggregates leads to increased activation of caspase-3, which was mediated by RAGE (Sousa *et al*. 2001a). When we posed the question whether ERK cascades could play a role in this process, we found that in fact blockade of ERK activation, using the MEK inhibitor U0126, abolished caspase-3 activation. These evidences point to ERK1/2 as an important player in mediating the cytotoxic effects of TTR aggregates.

Data with clinical samples revealed a chronic MEK-ERK activation starting at early asymptomatic stage (FAP 0) and persisting throughout the course of the disease. Moreover, in a FAP animal model, we show an increased ERK1/2 activation in total protein extracts of peripheral nerve from older mice (more prone to have TTR deposits) as compared with younger animals and control mice. The cellular localization of phosphorylated ERK (pERK) differed depending on the tissue analyzed. In FAP SG, pERK nuclear translocation was visualized. In FAP nerves, pERK was sequestered in axons where ERK acts in neuronal cytoplasmic substrates that might ultimately contribute to axon degeneration. The possibility of pERK nuclear translocation in dorsal root ganglia has to be considered, as TTR deposition in the stroma of sensitive ganglia most likely affects the cell body and probably leads to the nuclear regulation of specific gene products that then circulate in axons.

While ERK activation occurred at the asymptomatic and symptomatic levels both in SG and nerve, expression of the two phosphatases investigated differed. The down-regulation of MKP-1 (as shown by immunohistochemistry in SG and nerve, and microarray data) in symptomatic individuals correlated with the observed ERK up-regulation in the same tissues, but was not evident for the asymptomatic level. Immunohistochemical analysis of MKP-3 expression (a more specific ERK1/2 phosphatase as compared with the other MAPKs) differed between SG and nerves; while in SG, MKP-3 expression was down-regulated in accordance with the observed ERK activation in FAP 0 and FAP individuals, in nerves MKP-3 was overexpressed at the presymptomatic level (FAP 0). These results might derive from differences between the two tissues analyzed, including cell specific phosphatase expression and modulation which in FAP might have different responses at different clinical stages. It has been proposed that growth factors, cytokines, cell stressors or activated oncogenes induce MKPs gene transcription via both ERK-dependent and independent pathways (Camps *et al*. 2000; Colucci-D'Amato *et al*. 2003). In this context, active ERK can generate a negative feedback loop leading to the up-regulation of MKPs expression. Modulation of ERK activity by MKPs entails not only MKP expression level but also activity. In fact, recently, several phosphatases have been shown to be redox-sensitive and can be either reversibly or irreversibly inhibited, depending on the extension and mechanism of oxidation (Meng *et al*. 2002; Tonks 2003). Possible down-regulation of MKPs activity caused by oxidative stress, which occurs in FAP tissues both at the asymptomatic and symptomatic levels, can also modulate ERK activity.

Although ERK signaling pathways are generally thought to promote neuronal survival, there is a growing number of recent studies implicating ERK activation mediating neuronal injury. Neuronal cell lines and primary cultures exposed to oxidative stressors were protected by inhibition of ERK phosphorylation (Oh-hashi *et al*. 1999; Satoh *et al*. 2000; Stanciu *et al*. 2000; Kulich and Chu 2001). Moreover, animal models of cerebral ischemia-reperfusion treated with MEK inhibitors, developed neuroprotection (Alessandrini *et al*. 1999; Namura *et al*. 2001). In neurodegenerative diseases such as Alzheimer's disease (AD), Parkinson's disease (PD) and Lewy body dementias, pERK appears to be located within discrete, cytoplasmic granules (Pei *et al*. 2002; Zhu *et al*. 2002), and this pattern was also observed in 6-hydroxydopamine-treated neuronal cells (Zhu *et al*. 2002). Despite the existence of discrete active ERK accumulations in the cytoplasm, ERK may not be available to phosphorylate possible downstream pro-survival substrates. Conversely, substrates participating in pro-apoptotic pathways could be accessible to active ERK. For example, death associated protein kinase (DAPK) participates in various apoptotic paradigms and was shown to interact with ERK. ERK functions as the upstream activating kinase of DAPK, which promotes the cytoplasmic retention of ERK, thereby inhibiting ERK signaling in the nucleus and promoting DAPK activity (Chen *et al*. 2005).

The molecular signaling mechanisms in FAP neurodegeneration are not fully understood. In this study we pursued to unravel these signaling mechanisms and we found that ERK signaling cascade is abnormally activated. Finally, chronic ERK activation might be an early and sustained signaling amplifier of TTR deposits-induced cytotoxicity leading to NFkB activation, up-regulation of proinflammatory cytokines (i.e. IL-1β, TNFα, MCSF), oxidative stress, and ultimately to neurodegeneration in FAP.

Acknowledgements

We thank Paul Moreira for the production and purification of recombinant TTR, and Rui Fernandes (Advanced Tissue Analysis Facility, IBMC, Porto, Portugal) and Rossana Correia (Molecular Neurobiology, IBMC, Porto, Portugal) for tissue processing. This work was supported by grants from POCTI program of Fundação para a Ciência e Tecnologia – FCT, Saúde XXI and Gulbenkian Foundation, Portugal and fellowships SFRH/BPD/9416/2002 (to I. C) and SFRH/BD/4563/2001 (to F. A. M) from Fundação para a Ciência e Tecnologia, Portugal.

References

Alessandrini A., Namura S., Moskowitz M. A. and Bonventre J. V. (1999) MEK1 protein kinase inhibition protects against damage resulting from focal cerebral ischemia. *Proc. Natl Acad. Sci. USA* **96**, 12 866–12 869.

Almeida M. R., Damas A. M., Lans M. C., Brouwer A. and Saraiva M. J. (1997) Thyroxine binding to transthyretin Met 119. Comparative studies of different heterozygotic carriers and structural analysis. *Endocrine* **6**, 309–315.

Camps M., Nichols A. and Arkinstall S. (2000) Dual specificity phosphatases: a gene family for control of MAP kinase function. *FASEB J.* **14**, 6–16.

Chen C. H., Wang W. J., Kuo J. C., Tsai H. C., Lin J. R., Chang Z. F. and Chen R. H. (2005) Bidirectional signals transduced by DAPK–ERK interaction promote the apoptotic effect of DAPK. *EMBO J.* **24**, 294–304.

Coimbra A. and Andrade C. (1971a) Familial amyloid polyneuropathy: an electron microscope study of the peripheral nerve in five cases. II. Nerve fibre changes. *Brain* **94**, 207–212.

Coimbra A. and Andrade C. (1971b) Familial amyloid polyneuropathy: an electron microscope study of the peripheral nerve in five cases. I. Interstitial changes. *Brain* **94**, 199–206.

Colucci-D'Amato L., Perrone-Capano C. and di Porzio U. (2003) Chronic activation of ERK and neurodegenerative diseases. *Bioessays* **25**, 1085–1095.

Episkopou V., Maeda S., Nishiguchi S., Shimada K., Gaitanaris G. A., Gottesman M. E. and Robertson E. J. (1993) Disruption of the transthyretin gene results in mice with depressed levels of plasma retinol and thyroid hormone. *Proc. Natl Acad. Sci. USA* **90**, 2375–2379.

Grewal S. S., York R. D. and Stork P. J. (1999) Extracellular-signal-regulated kinase signalling in neurons. *Curr. Opin. Neurobiol.* **9**, 544–553.

Hanyu N., Ikeda S., Nakadai A., Yanagisawa N. and Powell H. C. (1989) Peripheral nerve pathological findings in familial amyloid polyneuropathy: a correlative study of proximal sciatic nerve and sural nerve lesions. *Ann. Neurol.* **25**, 340–350.

Hofer P. A. and Anderson R. (1975) Postmortem findings in primary familial amyloidosis with polyneuropathy. *Acta Pathol. Microbiol. Scand.* **83**, 309–322.

Huttunen H. J., Fages C. and Rauvala H. (1999) Receptor for advanced glycation end products (RAGE)-mediated neurite outgrowth and activation of NF-kappaB require the cytoplasmic domain of the receptor but different downstream signaling pathways. *J. Biol. Chem.* **274**, 19 919–19 924.

Ikeda S., Hanyu N., Hongo M., Yoshioka J., Oguchi H., Yanagisawa N., Kobayashi T., Tsukagoshi H., Ito N. and Yokota T. (1987) Hereditary generalized amyloidosis with polyneuropathy. Clinicopathological study of 65 Japanese patients. *Brain* **110**, 315–337.

Ishihara K., Tsutsumi K., Kawane S., Nakajima M. and Kasaoka T. (2003) The receptor for advanced glycation end-products (RAGE) directly binds to ERK by a D-domain-like docking site. *FEBS Lett.* **550**, 107–113.

Kohno K., Palha J. A., Miyakawa K., Saraiva M. J., Ito S., Mabuchi T., Blaner W. S., Iijima H., Tsukahara S., Episkopou V., Gottesman M. E., Shimada K., Takahashi K., Yamamura K. and Maeda S. (1997) Analysis of amyloid deposition in a transgenic mouse model of homozygous familial amyloidotic polyneuropathy. *Am. J. Pathol.* **150**, 1497–1508.

Kulich S. M. and Chu C. T. (2001) Sustained extracellular signal-regulated kinase activation by 6-hydroxydopamine: implications for Parkinson's disease. *J. Neurochem.* **77**, 1058–1066.

Lander H. M., Tauras J. M., Ogiste J. S., Hori O., Moss R. A. and Schmidt A. M. (1997) Activation of the receptor for advanced glycation end products triggers a p21 (ras)-dependent mitogen-activated protein kinase pathway regulated by oxidant stress. *J. Biol. Chem.* **272**, 17 810–17 814.

Li J. and Schmidt A. M. (1997) Characterization and functional analysis of the promoter of RAGE, the receptor for advanced glycation end products. *J. Biol. Chem.* **272**, 16 498–16 506.

Lowry O. H., Rosebrough N. J., Farr A. L. and Randall R. J. (1951) Protein measurement with the Folin phenol reagent. *J. Biol. Chem.* **193**, 265–275.

Meng T. C., Fukada T. and Tonks N. K. (2002) Reversible oxidation and inactivation of protein tyrosine phosphatases in vivo. *Mol. Cell.* **9**, 387–399.

Namura S., Iihara K., Takami S., Nagata I., Kikuchi H., Matsushita K., MoskowitZ. M. A., Bonventre J. V. and Alessandrini A. (2001) Intravenous administration of MEK inhibitor U0126 affords brain protection against forebrain ischemia and focal cerebral ischemia. *Proc. Natl Acad. Sci. USA* **98**, 11 569–11 574.

Oh-hashi K., Maruyama W., Yi H., Takahashi T., Naoi M. and Isobe K. (1999) Mitogen-activated protein kinase pathway mediates peroxynitrite-induced apoptosis in human dopaminergic neuroblastoma SH-SY5Y cells. *Biochem. Biophys. Res. Commun.* **263**, 504–509.

Pearson G., Robinson F., Beers Gibson T., Xu B. E., Karandikar M., Berman K. and Cobb M. H. (2001) Mitogen-activated protein (MAP) kinase pathways: regulation and physiological functions. *Endocr. Rev.* **22**, 153–183.

Pei J. J., Braak H., An W. L., Winblad B., Cowburn R. F., Iqbal K. and Grundke-Iqbal I. (2002) Up-regulation of mitogen-activated protein kinases ERK1/2 and MEK1/2 is associated with the progression of neurofibrillary degeneration in Alzheimer's disease. *Brain Res. Mol. Brain. Res.* **109**, 45–55.

Rong L. L., Yan S. F., Wendt T., Hans D., Pachydaki S., Bucciarelli L. G., Adebayo A., Qu W., Lu Y., Kostov K., Lalla E., Yan S. D., Gooch C., Szabolcs M., Trojaborg W., Hays A. P. and Schmidt A. M. (2004) RAGE modulates peripheral nerve regeneration via recruitment of both inflammatory and axonal outgrowth pathways. *FASEB J.* **18**, 1818–1825.

Satoh T., Nakatsuka D., Watanabe Y., Nagata I., Kikuchi H. and Namura S. (2000) Neuroprotection by MAPK/ERK kinase inhibition with U0126 against oxidative stress in a mouse neuronal cell line and rat primary cultured cortical neurons. *Neurosci. Lett.* **288**, 163–166.

Sousa M. M., Cardoso I., Fernandes R., Guimaraes A. and Saraiva M. J. (2001b) Deposition of transthyretin in early stages of familial amyloidotic polyneuropathy: evidence for toxicity of nonfibrillar aggregates. *Am. J. Pathol.* **159**, 1993–2000.

Sousa M. M., do Amaral J. B., Guimaraes A. and Saraiva M. J. (2005) Up-regulation of the extracellular matrix remodeling genes, biglycan, neutrophil gelatinase-associated lipocalin, and matrix metalloproteinase-9 in familial amyloid polyneuropathy. *FASEB J.* **19**, 124–126.

Sousa M. M., Du Yan S., Fernandes R., Guimaraes A., Stern D. and Saraiva M. J. (2001a) Familial amyloid polyneuropathy: receptor for advanced glycation end products-dependent triggering of neuronal inflammatory and apoptotic pathways. *J. Neurosci.* **21**, 7576–7586.

Sousa M. M., Yan S. D., Stern D. and Saraiva M. J. (2000) Interaction of the receptor for advanced glycation end products (RAGE) with transthyretin triggers nuclear transcription factor kB (NF-kB) activation. *Laboratory Invest.* **80**, 1101–1110.

Stanciu M., Wang Y., Kentor R., Burke N., Watkins S., Kress G., Reynolds I., Klann E., Angiolieri M. R., Johnson J. W. and DeFranco D. B. (2000) Persistent activation of ERK contributes to glutamate-induced oxidative toxicity in a neuronal cell line and primary cortical neuron cultures. *J. Biol. Chem.* **275**, 12 200–12 206.

Taguchi A., Blood D. C., del Toro G., Canet A., Lee D. C., Qu W., Tanji N., Lu Y., Lalla E., Fu C., Hofmann M. A., Kislinger T., Ingram M., Lu A., Tanaka H., Hori O., Ogawa S., Stern D. M. and Schmidt A. M. (2000) Blockade of RAGE-amphoterin signalling suppresses tumour growth and metastases. *Nature* **405**, 354–360.

Takahashi K., Yi S., Kimura Y. and Araki S. (1991) Familial amyloidotic polyneuropathy type 1 in Kumamoto, Japan: a clinicopathologic, histochemical, immunohistochemical, and ultrastructural study. *Hum. Pathol.* **22**, 519–527.

Takaoka Y., Tashiro F., Yi S., Maeda S., Shimada K., Takahashi K., Sakaki Y. and Yamamura K. (1997) Comparison of amyloid deposition in two lines of transgenic mouse that model familial amyloidotic polyneuropathy, type I. *Transgenic Res.* **6**, 261–269.

Tonks N. K. (2003) PTP1B: from the sidelines to the front lines. *FEBS Lett.* **546**, 140–148.

Yan S. D., Schmidt A. M., Anderson G. M., Zhang J., Brett J., Zou Y. S., Pinsky D. and Stern D. (1994) Enhanced cellular oxidant stress by the interaction of advanced glycation end products with their receptors/binding proteins. *J. Biol. Chem.* **269**, 9889–9897.

Zhu J. H., Kulich S. M., Oury T. D. and Chu C. T. (2002) Cytoplasmic aggregates of phosphorylated extracellular signal-regulated protein kinases in Lewy body diseases. *Am. J. Pathol.* **161**, 2087–2098.

